Mutual Antagonism of Target of Rapamycin and Calcineurin Signaling[*]

Jose M. Mulet[1]**, Dietmar E. Martin, Robbie Loewith**[2]**, and Michael N. Hall**[3]

From the Biozentrum, University of Basel, Klingelbergstrasse 70, CH 4056 Basel, Switzerland

Growth and stress are generally incompatible states. Stressed cells adapt to an insult by restraining growth, and conversely, growing cells keep stress responses at bay. This is evident in many physiological settings, including for example, the effect of stress on the immune or nervous system, but the underlying signaling mechanisms mediating such mutual antagonism are poorly understood. In eukaryotes, a central activator of cell growth is the protein kinase target of rapamycin (TOR) and its namesake signaling network. Calcineurin is a conserved, Ca^{2+}/calmodulin-dependent protein phosphatase and target of the immunosuppressant FK506 (tacrolimus) that is activated in yeast during stress to promote cell survival. Here we show yeast mutants defective for TOR complex 2 (TORC2) or the essential homologous TORC2 effectors, SLM1 and SLM2, exhibited constitutive activation of calcineurin-dependent transcription and actin depolarization. Conversely, cells defective in calcineurin exhibited SLM1 hyperphosphorylation and enhanced interaction between TORC2 and SLM1. Furthermore, a mutant SLM1 protein (SLM1$^{\Delta C14}$) lacking a sequence related to the consensus calcineurin docking site (PxIxIT) was insensitive to calcineurin, and *SLM1$^{\Delta C14}$ slm2* mutant cells were hypersensitive to oxidative stress. Thus, TORC2-SLM signaling negatively regulates calcineurin, and calcineurin negatively regulates TORC2-SLM. These findings provide a molecular basis for the mutual antagonism of growth and stress.

TOR[5] is a serine/threonine kinase and a central controller of cell growth. TOR is found in two structurally and functionally distinct, evolutionarily conserved protein complexes, TORC1 and TORC2 (1–3). TORC1 is rapamycin-sensitive and controls several growth-related processes including transcription, translation, ribosome biogenesis, nutrient transport, and autophagy in response to nutrient, energy, and (in metazoans) growth factor signals (3). TORC2 is rapamycin-insensitive and controls polarization of the actin cytoskeleton via a ROM2-RHO-PKC1-MPK1/SLT2 effector pathway (4, 5). Thus, TOR via its two complexes integrates temporal and spatial control of cell growth.

In the yeast *Saccharomyces cerevisiae*, calcineurin promotes cell survival upon environmental stress (6). In response to a stress-induced increase in cytoplasmic calcium, calcineurin dephosphorylates and activates several cytoplasmic targets. The calcineurin docking site in target proteins consists of the consensus sequence PxIxIT. The best characterized calcineurin target in yeast is the transcription factor CRZ1/TCN1/HAL8 (7–9). Dephosphorylated CRZ1 translocates into the nucleus and activates target genes containing a calcineurin-dependent response element. These genes are involved mainly in ion homeostasis, vesicular transport, and cell wall maintenance. Independent of transcription, calcineurin also mediates stress-induced depolarization of the actin cytoskeleton and a delay in the G_2–M transition of the cell cycle (10, 11). Calcineurin is a heterodimer composed of a positive regulatory subunit (CNB1) and in *S. cerevisiae*, one of the redundant catalytic subunits CNA1 and CNA2.

Cells respond to environmental stress by down-regulating energy demanding growth processes and up-regulating survival processes. How do cells counter-regulate growth and stress responses? A functional interaction between calcineurin and TOR has been suggested by a two-hybrid interaction between CNA (CNA1 or CNA2) and the TORC2 phosphorylation substrates SLM1 and SLM2 (12). The homologous SLM1 and SLM2 are redundant, essential proteins that control polarization of the actin cytoskeleton by an unknown mechanism (13, 14). In this study we show that TORC2 and calcineurin inhibit each other via the SLM proteins. Our findings provide a molecular mechanism for the mutual antagonism of growth-promoting and growth-inhibiting signaling pathways. Furthermore, we show that TORC2 controls transcription and has a pivotal role in the negative regulation of calcineurin-dependent stress signaling, in addition to controlling organization of the actin cytoskeleton.

EXPERIMENTAL PROCEDURES

Strains, Plasmids, and Media—The *S. cerevisiae* strains and plasmids used in this study are listed in Table 1. All strains are isogenic derivatives of TB50 or JK9-3d. Medium (YPD/YPGal) was prepared as described previously (15, 16). YPD containing 0.2 M $CaCl_2$ was prepared by adding the required volume of a 1 M stock of $CaCl_2$ to 1.25-fold concentrated, autoclaved YPD. FK506 was added to a final concentration of

TABLE 1

All strains are *S. cerevisiae*. Unless otherwise indicated, all the strains were constructed for this study

Strain	Genotype	Source
JK9-3da	MATa *leu2-3,112 ura3-52 trp1 his4 rme HMLa*	
JM229	TB50a *CNA1-3HA-[His3MX6]*	
JM256	TB50a *crz1::HIS3*	
JM259	TB50a *CNA1-3HA-[His3MX6] SLM1-13myc-[kanMX6]*	
JM262	TB50a *CRZ1-13myc-[His3MX6]*	
JM270	TB50a *[His3MX6]-GAL1p-SLM2 slm1::kanMX6 CRZ1-13myc-[His3MX6]*	
JM271	TB50a *[His3MX6]-GAL1p-SLM2 slm1::kanMX6 crz1::HIS3*	
JM304	TB50a *cnb1::His3MX6*	
JM316	TB50α *cnb1::His3MX6*	
JM321	TB50a *[His3MX6]-GAL1p-AVO3 crz1::HIS3*	
JM324	TB50a *[His3MX6]-GAL1p-AVO3 CRZ1-13myc-[His3MX6]*	
JM333	TB50a *SLM1-TAP-[kanMX6] cnb1::His3MX6*	
JM338	TB50a *[His3MX6]-GAL1p-TOR2 crz1::HIS3*	
JM340	TB50a *[His3MX6]-GAL1p-TOR2 CRZ1-13myc-[His3MX6]*	
JM345	TB50a *[His3MX6]-GAL1p-TOR2*	
JM347	TB50a *[His3MX6]-GAL1p-AVO3*	
JM474	TB50a *[His3MX6]-GAL1p-SLM2 slm1::kanMX6 cnb1::His3MX6*	
JM481	TB50a *AVO3-3HA-[kanMX6] SLM1-13myc-[kanMX6] cnb1::His3MX6*	
JM491	TB50a *SLM1-13myc-[kanMX6] CNA1-3HA-[His3MX6] cnb1::His3MX6*	
JM501	TB50a *[His3MX6]-GAL1p-TOR2 cnb1::His3MX6*	
JM597	TB50a *SLM1^{ΔC14}-TAP-[His3MX6]*	
JM611	TB50a *SLM1^{ΔC14}-TAP-[His3MX6] slm2::kanMX6*	
JM624	TB50a *SLM1^{ΔC14}-13myc-[His3MX6] CNA1-3HA-[His3MX6] cnb1::His3MX6*	
JM626	TB50a *SLM1^{ΔC14}-13myc-[His3MX6] AVO3-3HA-[kanMX6]*	
JM712	TB50a *SLM1^{ΔC14}-TAP-[His3MX6] cnb1::His3MX6*	
JM717	TB50a *SLM1^{ΔC14}-TAP-[His3MX6] crz1::HIS3*	
RL42-1c	TB50a *AVO3-3HA-[kanMX6]*	
RL136-1a	TB50α *slm2::kanMX6*	
RL146-7d	TB50a *SLM1-13myc-[kanMX6]*	
RL164-2b	TB50a *AVO3-3HA-[kanMX6] SLM1-13myc-[kanMX6]*	
RL202-5a	TB50a *[His3MX6]-GAL1p-SLM2 slm1::kanMX6*	
RL209	TB50a *SLM1-TAP-[kanMX6]*	
SH100	JK9-3da *tor2::ADE2-3/YCplac111::TOR2*	Ref. 19
SH121	JK9-3da *tor2::ADE2-3/YCplac111::tor2-21^{ts}*	Ref. 19
TB50a	JK9-3da *HIS4 his3*	Hall lab.

2 µg/ml from a 1 mg/ml stock in 90% ethanol-10% Tween 20. FK506 treatment was for 30 min. H_2O_2 was added from a 30% commercial solution (Fluka) to autoclaved YPD agar medium prior to solidification to a final concentration of 5 mM. For TOR2-, AVO3-, and SLM2-depletion experiments, YPGal cultures of logarithmically growing cells, conditionally expressing the corresponding genes from the *GAL1* promoter, were inoculated into YPD medium and incubated with aeration for 15 (TOR2 or AVO3 depletion) or 6 h (SLM2 depletion). The long incubation times reflect the amount of time required to deplete the proteins in question (17). PCR cassettes were used to generate gene deletions and epitope tags in the genome as described previously (18). An SLM mutant lacking the PxIxIT-related, putative calcineurin docking site was constructed by replacing the C-terminal 14 amino acids of SLM1 with a Myc or TAP tag in the genome as described above.

RNA Isolation, Microarray, and Northern Blot Analysis—For the microarray experiment, *S. cerevisiae* strains SH100 and SH121 (19) were grown at nonpermissive temperature (37 °C) for 6 h, as described (20). Total RNA was extracted using a hot phenol method essentially as described (21). Affymetrix^TM S98 Yeast Genome GeneChips, containing 6,400 *S. cerevisiae* (S288C strain) genes, were used. Two independent RNA preparations were used for each strain. Quantity and quality of total RNA were determined by capillary electrophoresis on a RNA6000 Bioanalyzer (Agilent Technologies). Synthesis of cDNA, *in vitro* transcription of biotin-labeled cRNA, microarray hybridization, washing, and staining procedures were carried out according to standard protocols as recommended by the manufacturer (Affymetrix). Data normalization was performed using the Robust Multi-array Analysis algorithm as implemented in GeneSpring 7.2 software. For Northern blot analysis, probe synthesis was performed by PCR using digoxygenin-modified dUTP, and subsequent Northern blot analysis was performed according to the manufacturer's protocol (digoxygenin labeling and detection, Roche).

Coimmunoprecipitation, TAP Purification, and Immunoblotting—Coimmunoprecipitations and the TAP pulldown assays were performed as described (17). HA- and Myc-tagged proteins were precipitated or detected with mouse anti-HA antibody (clone 12CA5) or mouse anti-Myc antibody (clone 9E10). Phospho-SLM1-TAP was detected by immunoblotting with anti-phosphothreonine (Q7, Qiagen) and anti-phosphoserine (Q5, Qiagen) antibodies. Total SLM1-TAP was detected with anti-TAP (protein A) antibody. Horseradish peroxidase-conjugated anti-mouse antibody and ECL reagents were used for immunoblots (Amersham Biosciences). Proteins coprecipitating in TAP pulldowns were excised from a 5–20% gradient gel and identified by mass spectrometry as described (1).

In Vitro Calcineurin Assay—Phospho-SLM1-TAP was purified for use as a calcineurin substrate by TAP pull down from an extract prepared from JM333 yeast cells (*cnb1*) as described (17) but using TL buffer (40 mM Tris-HCl, pH 7.5, 100 mM KCl, 1 mM $MgCl_2$, 250 mM sorbitol, 1 mM dithiothreitol, 0.1% Nonidet P-40) instead of phosphate-buffered saline buffer. The slurry of IgG beads containing SLM1-TAP was washed with CP buffer (50 mM Tris-HCl, pH 7.5, 1 mM $MgCl_2$, 1 mM dithiothreitol) containing protease inhibitors. The calcineurin reaction

A

Venn diagram:
121 | **42** | **45**

Calcineurin/CRZ1 dependent genes | **Genes up-regulated in *tor2^ts***

B

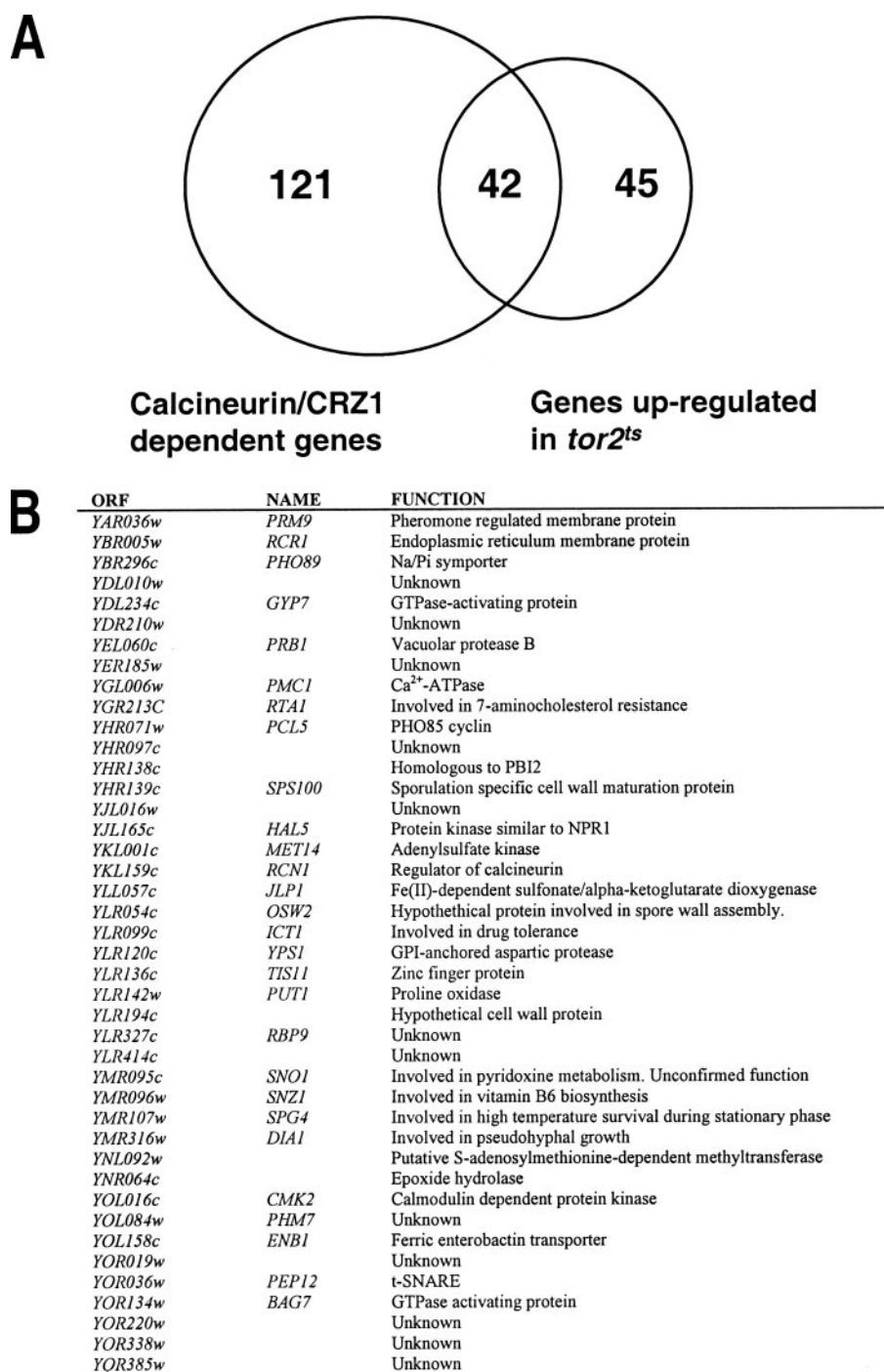| ORF	NAME	FUNCTION
YAR036w	*PRM9*	Pheromone regulated membrane protein
YBR005w	*RCR1*	Endoplasmic reticulum membrane protein
YBR296c	*PHO89*	Na/Pi symporter
YDL010w		Unknown
YDL234c	*GYP7*	GTPase-activating protein
YDR210w		Unknown
YEL060c	*PRB1*	Vacuolar protease B
YER185w		Unknown
YGL006w	*PMC1*	Ca^{2+}-ATPase
YGR213C	*RTA1*	Involved in 7-aminocholesterol resistance
YHR071w	*PCL5*	PHO85 cyclin
YHR097c		Unknown
YHR138c		Homologous to PBI2
YHR139c	*SPS100*	Sporulation specific cell wall maturation protein
YJL016w		Unknown
YJL165c	*HAL5*	Protein kinase similar to NPR1
YKL001c	*MET14*	Adenylsulfate kinase
YKL159c	*RCN1*	Regulator of calcineurin
YLL057c	*JLP1*	Fe(II)-dependent sulfonate/alpha-ketoglutarate dioxygenase
YLR054c	*OSW2*	Hypothetical protein involved in spore wall assembly.
YLR099c	*ICT1*	Involved in drug tolerance
YLR120c	*YPS1*	GPI-anchored aspartic protease
YLR136c	*TIS11*	Zinc finger protein
YLR142w	*PUT1*	Proline oxidase
YLR194c		Hypothetical cell wall protein
YLR327c	*RBP9*	Unknown
YLR414c		Unknown
YMR095c	*SNO1*	Involved in pyridoxine metabolism. Unconfirmed function
YMR096w	*SNZ1*	Involved in vitamin B6 biosynthesis
YMR107w	*SPG4*	Involved in high temperature survival during stationary phase
YMR316w	*DIA1*	Involved in pseudohyphal growth
YNL092w		Putative S-adenosylmethionine-dependent methyltransferase
YNR064c		Epoxide hydrolase
YOL016c	*CMK2*	Calmodulin dependent protein kinase
YOL084w	*PHM7*	Unknown
YOL158c	*ENB1*	Ferric enterobactin transporter
YOR019w		Unknown
YOR036w	*PEP12*	t-SNARE
YOR134w	*BAG7*	GTPase activating protein
YOR220w		Unknown
YOR338w		Unknown
YOR385w		Unknown

FIGURE 1. **Microarray analysis of a *tor2* mutant defective in TORC2.** *A*, summary of DNA microarray analysis. Genes induced in a calcineurin/CRZ1-dependent manner (24) and those induced in a *tor2^ts* mutant are compared. *B*, names and brief descriptions of the genes included in the diagram intersection in *A*. Raw microarray data files can be found in the NCBI GEO repository under the series number GSE1814.

described (23). An anti-Myc (9E10) antibody was used to visualize CRZ1-Myc. Control experiments with wild type cells showed that the unspecific signal was negligible in our strain. For actin cytoskeleton or DNA staining, we used a modification of the method described in (1), eliminating the phosphate buffer to avoid calcium phosphate precipitation. Cells from the indicated YPD cultures were fixed in formaldehyde (3.7%) and stained with tetramethyl rhodamine isothiocyanate-phalloidin (Sigma) to visualize actin or 4′,6-diamidino-2-phenylindole to stain DNA and visualize nuclei. Actin cytoskeleton organization was assessed in several hundred cells as described (19).

RESULTS

TORC2 Negatively Controls Calcineurin-dependent Transcription—TORC2, because of its rapamycin insensitivity, is less well characterized than TORC1. To further investigate TORC2, we performed a genome-wide transcriptome analysis on an *S. cerevisiae* strain (SH121) containing the thermosensitive *tor2–21* (*tor2^ts*) allele (19). This strain is defective for TORC2 but not for TORC1 (1, 17). At nonpermissive temperature, ~90 genes were up-regulated (≥2-fold induction), and no genes were significantly down-regulated in the *tor2^ts* mutant, compared with wild type (Fig. 1). This suggests that TORC2 controls transcription, mainly negatively. Further analysis revealed that ~50% of the genes inhibited by TORC2 overlapped with a set of genes, the expression of which was dependent on calcineurin and CRZ1 (24) (Fig. 1). The overlapping genes include those most dependent on calcineurin and CRZ1 for expression (≥5.5-fold induction upon calcineurin activation). These findings suggest that TORC2 inhibits calcineurin and CRZ1.

To determine whether TORC2 indeed inhibits CRZ1, we examined CRZ1-dependent transcription directly in a *tor2* mutant and in a mutant defective for the TORC2-specific subunit AVO3. Transcripts corresponding to the CRZ1 target genes *CMK2*, *DIA1*, *YLR194c*, and *YOR385w* were probed by Northern analysis in strains conditionally expressing *TOR2* or *AVO3* from the galactose-inducible and
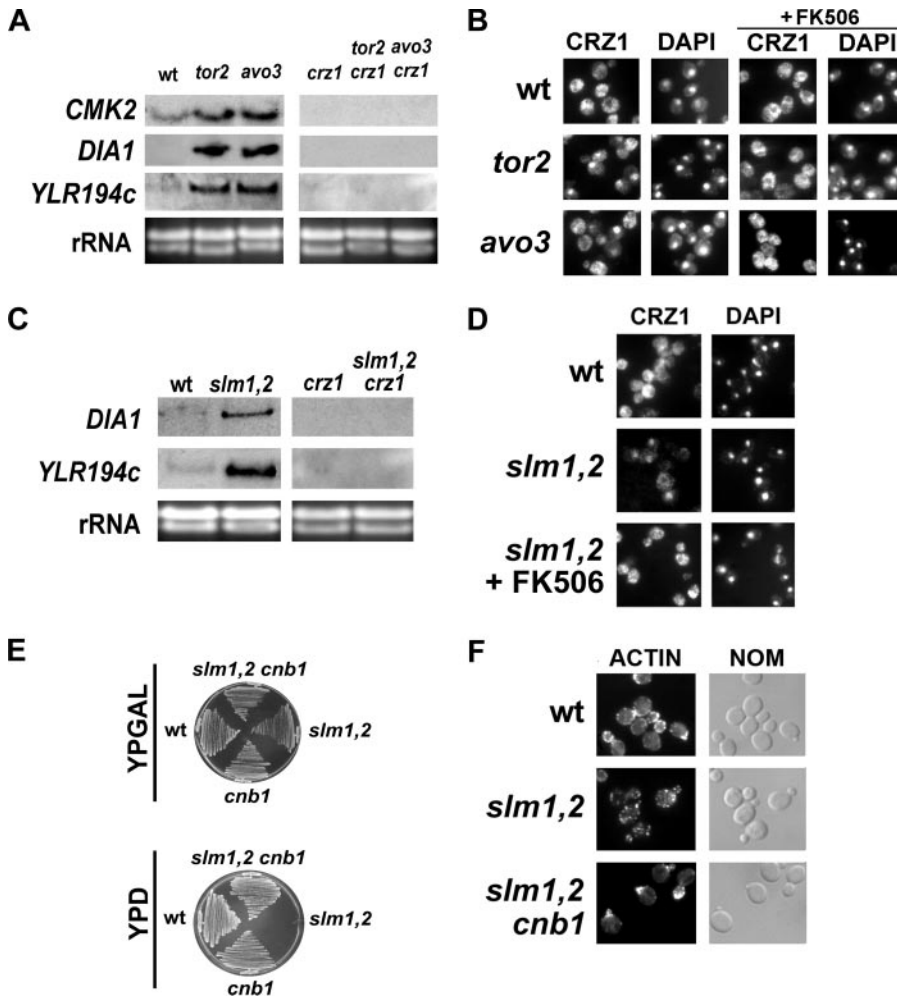
was performed in a total volume of 100 μl in CP buffer containing 500 units of recombinant human calcineurin (Calbiochem) and 2600 units of calmodulin (Sigma) as described (22). Where indicated, CaCl$_2$ and EGTA were added to a final concentration of 40 and 10 mM, respectively. Phosphatase reactions were incubated at 30 °C for 30 min. Phospho-SLM1-TAP and total SLM1-TAP were detected as described above.

Microscopy—Florescence microscopy and indirect immunofluorescence imaging on whole fixed cells were performed as

FIGURE 2. **TORC2 negatively regulates calcineurin and CRZ1 via the SLM proteins.** *A*, CRZ1-dependent transcription is constitutively activated in TORC2 mutants. Transcripts of the indicated CRZ1 target genes were visualized in the indicated strains, wt (TB50**a**), *tor2* (JM345), *avo3* (JM347), *crz1* (JM256), *tor2 crz1* (JM338), *avo3 crz1* (JM321), by Northern analysis. *B*, the calcineurin-dependent transcription factor CRZ1 localizes to the nucleus in *tor2* and *avo3* mutant. This constitutive localization is abolished upon inhibition of calcineurin by addition of FK506 to cells. CRZ1 localization (*CRZ1*) was examined in the following strains: wt (JM262), *tor2* (JM340), and *avo3* (JM324). In all cases, a monoclonal anti-Myc antibody was used as a primary antibody for indirect immunofluorescence. DNA was stained with 4′,6-diamidino-2-phenylindole to visualize nuclei. *C*, CRZ1-dependent transcription is constitutively activated in *slm1,2* mutants. Transcripts of the indicated CRZ1 target genes were visualized in the indicated strains, wt (TB50**a**), *slm1,2* (RL202-5a), *crz1* (JM256), *slm1,2 crz1* (JM271), by Northern analysis. *D*, the calcineurin-dependent transcription factor CRZ1 localizes to the nucleus in a *slm1,2* mutant. This constitutive localization is abolished upon inhibition of calcineurin by addition of FK506 to cells. CRZ1 localization (CRZ1) was examined in a wt (JM262) and in a *slm1,2* mutant (JM270). In all cases, a monoclonal anti-Myc antibody was used as a primary antibody for indirect immunofluorescence. DNA was stained with 4′,6-diamidino-2-phenylindole to visualize nuclei. *E*, deletion of the regulatory subunit of calcineurin (CNB1) suppresses the lethality of a conditional *slm1,2* mutant. Strain *slm1,2 cnb1* (JM474) was constructed by crossing strain *slm1,2* (RL202-5a) with *cnb1* (JM316) and selecting strains with the appropriate markers. Growth of the indicated strains was tested on permissive (*YPGal*) and nonpermissive (*YPD*) medium by incubating the different plates for 3 days at 30 °C. *F*, *CNB1* mutation suppresses the actin depolarization phenotype of a *slm1 slm2* double mutant (*slm1,2*). Strains described in *E* were grown in restrictive (*YPD*) medium to mid-logarithmic phase, fixed, and stained for F-actin using rhodamine-phalloidin (*ACTIN*). Cells were visualized using Nomarski optics (*NOM*).

(Fig. 2*A*). We also observed calcineurin-dependent response element (CDRE)-dependent expression of *lacZ* upon TOR2 or AVO3 depletion (data not shown). These experiments confirm the results of the transcriptome analysis with the *tor2*[ts] mutant and indicate that the expression changes observed with the *tor2*[ts] mutant are not necessarily because of heat stress. Thus, TORC2 inhibits CRZ1-dependent transcription under normal growth conditions, *i.e.* in the absence of stress.

Calcineurin dephosphorylates CRZ1 and thereby triggers nuclear localization and activation of CRZ1 (25). To investigate whether TORC2 regulates calcineurin, we examined CRZ1 localization in the *tor2* and *avo3* mutants by indirect immunofluorescence on whole fixed cells (Fig. 2*B*). In both *tor2* and *avo3* mutant cells, CRZ1 was exclusively (15–20% of cells) or mainly (45–50% of cells) nuclear, whereas in wild type cells CRZ1 was exclusively or mainly cytoplasmic. Thus, TORC2 inhibits nuclear accumulation of CRZ1. To investigate the calcineurin-dependence of CRZ1 nuclear localization in the *tor2* and *avo3* mutants, cells were treated with the calcineurin inhibitor FK506. A short treatment (30 min) with FK506 restored cytoplasmic localization of CRZ1 in *tor2* and *avo3* cells (Fig. 2*B*). Similar suppression of the CRZ1 localization defect was obtained upon deletion of *CNB1* encoding the positive regulatory subunit of calcineurin (data not shown). Thus, CRZ1 nuclear localization in the *tor2* and *avo3* mutants was calcineurin-dependent. The above findings suggest that TORC2 negatively regulates calcineurin. However, these experiments do not distinguish whether the TORC2 inhibits calcineurin directly or indirectly.

TORC2 Inhibits Calcineurin via the SLM Proteins—The observation that the TORC2 substrates SLM1 and SLM2 interact with the catalytic subunit of calcineurin (CNA1 or CNA2), as revealed by a genome-wide two-hybrid study (12), suggests that TORC2 inhibits calcineurin via the SLMs. To investigate this possibility, we examined CRZ1-dependent transcription and CRZ1 localization in a *slm1 slm2* double mutant (*slm1,2*).
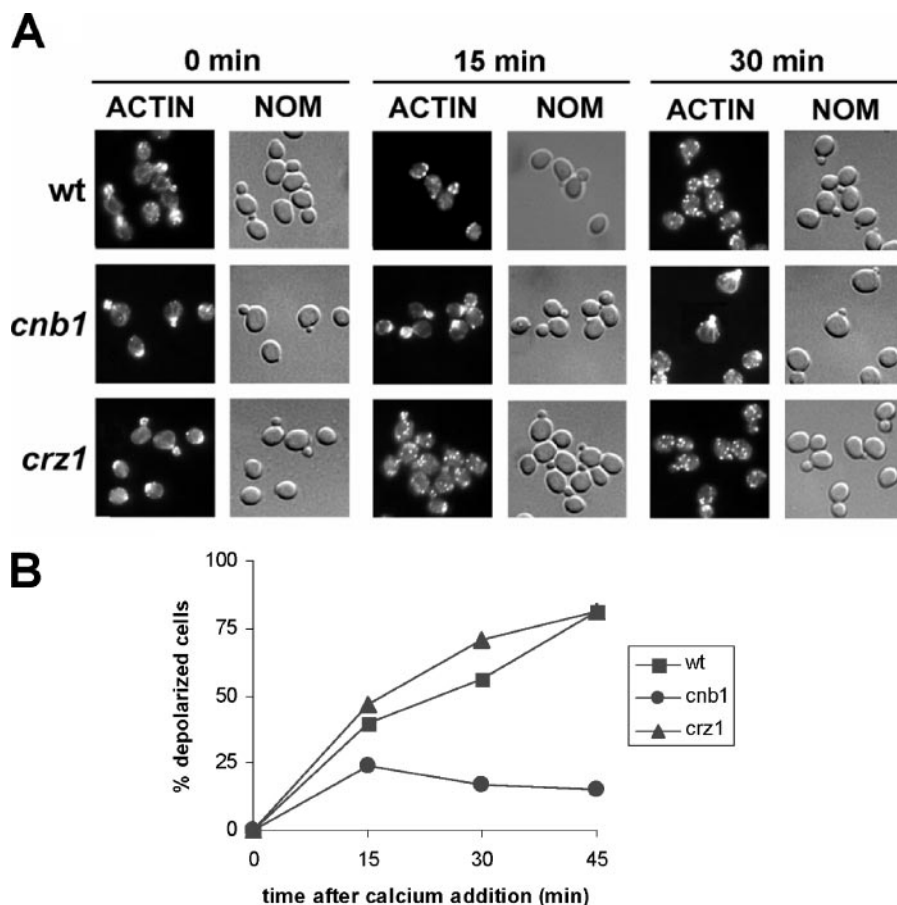
glucose-repressible *GAL1* promoter. Strains conditionally expressing *TOR2* or *AVO3* were used, instead of strains containing a thermosensitive *tor2* or *avo3* allele, to avoid potential complications because of heat stress activation of CRZ1. The CRZ1 target genes were induced upon depletion of TOR2 or AVO3 and in the absence of any other stress (Fig. 2*A*; data not shown for *YOR385w*). The CRZ1 dependence of the examined transcripts was determined by deleting *CRZ1* in the *tor2* and *avo3* strains

FIGURE 3. **Calcineurin mediates depolarization of the actin cytoskeleton independently of CRZ1.** *A*, wt (TB50**a**), *cnb1* (JM304), and *crz1* (JM256) cells were grown in YPD medium until mid-logarithmic phase and then transferred to fresh medium containing 0.2 M CaCl$_2$ to activate calcineurin. At the indicated times, aliquots were removed, fixed, and stained for F-actin using rhodamine-phalloidin (*ACTIN*). Cells were visualized using Nomarski optics (*NOM*). *B*, quantitation of the actin depolarization induced by calcium. Small to medium budded cells (≈200) of wild type (*squares*), *cnb1* (*circles*), and *crz1* (*triangles*) strains were scored for their actin polarization state. Similar results were obtained in three separate experiments.

RHO2 also failed to suppress the CRZ1 nuclear localization phenotype of the *tor2* mutant (data not shown). These observations suggest that TORC2 signals via SLM-calcineurin and ROM2-RHO-PKC-MPK1/SLT2 separately.

Calcineurin Antagonizes TORC2-SLM Signaling—TORC2 positively controls polarization of the actin cytoskeleton. In contrast, activation of calcineurin causes depolarization of the actin cytoskeleton (Fig. 2*F* and Fig. 3). Furthermore, calcineurin causes depolarization of the actin cytoskeleton independently of CRZ1 (Fig. 3). These observations suggest that calcineurin may antagonize the ability of TORC2 to signal via the SLMs. To address this suggestion, we first investigated whether calcineurin (CNA1) interacts with SLM1 as suggested previously by a genome-wide two-hybrid analysis (12). Our efforts to detect, by coimmunoprecipitation, an SLM1-CNA1 interaction in a wild type strain were unsuccessful. As this could be because of CNA1 dephosphorylating and thereby releasing SLM1, we then investigated an SLM1-CNA1 interaction under conditions in which calcineurin was inactive. Inhibition of calcineurin by a *cnb1* mutation or by treatment of cells with FK506 indeed resulted in detection of an SLM1-CNA1 interaction (Fig. 4*A*) (data not shown for FK506). To study further the SLM1-CNA1 interaction, we examined whether SLM1 contained a PxIxIT calcineurin docking site. Although we did not detect a consensus PxIxIT sequence, a related sequence (PNIYIQ) was detected in the C-terminal 14 amino acids of SLM1 (PNIYIQ TPINDFKS). To determine whether this PxIxIT-related sequence is a calcineurin docking site, the C-terminal 14 amino acids of SLM1 were deleted, and the truncated protein (SLM1$^{\Delta C14}$) was assayed by coimmunoprecipitation for interaction with CNA1. SLM1$^{\Delta C14}$ failed to interact with CNA1 even upon inhibition of calcineurin (Fig. 4*A*), suggesting that the PxIxIT-related sequence in SLM1 was a calcineurin binding site. The SLM1$^{\Delta C14}$ mutant protein was functional other than in its ability to interact with CNA1 because a *SLM1$^{\Delta C14}$ slm2* double mutant grew like a wild type strain under standard growth conditions, unlike the *slm1 slm2* double mutant (*slm1,2*), which was nonviable (data not shown). The above findings indicate that calcineurin interacts directly with SLM1. Interestingly, the observation that SLM1$^{\Delta C14}$ is functional despite its inability to interact with calcineurin suggests that SLM1 has a function independent of its direct interaction with calcineurin.
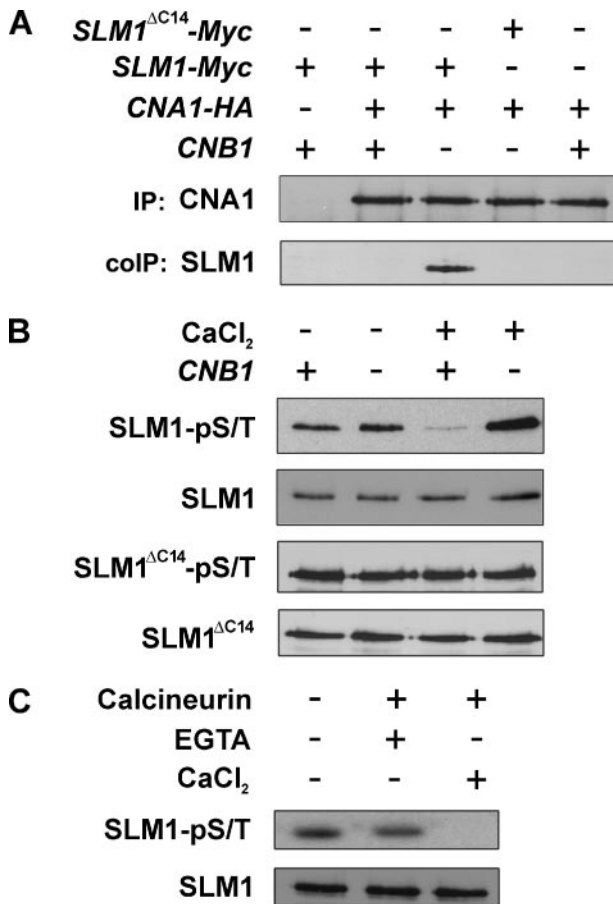
Because the SLMs are essential, strains containing a *SLM1* deletion and conditionally expressing *SLM2* from the *GAL1* promoter were used for these experiments. In a *slm1,2* mutant, CRZ1 accumulated in the nucleus in a calcineurin-dependent (FK506 sensitive) manner and activated transcription of target genes (data not shown for *YOR385w*) even in the absence of stress (Fig. 2, *C* and *D*). In addition, inhibition of calcineurin by treatment with FK506 or by deletion of *CNB1* suppressed the growth and actin defects of a *slm1,2* mutant (Fig. 2, *E* and *F*). Thus, calcineurin appears to be constitutively active in a *slm1,2* mutant, like in TORC2 mutants (*tor2* and *avo3*) and the cause of lethality of a *slm1,2* mutation. These observations suggest that TORC2 negatively regulates calcineurin via the SLMs. Furthermore, the suppression of the *slm1,2* actin defect by *CNB1* deletion or by FK506 treatment suggests that the SLMs mediate actin polarization via inhibition of calcineurin.

Interestingly, inhibition of calcineurin did not suppress the lethality of a *tor2* or *avo3* mutation (data not shown). Furthermore, multicopy *ROM2* or *RHO2*, strong suppressors of *tor2* or *avo3* lethality (1, 4), failed to suppress either the growth defect or the CRZ1 nuclear localization phenotype of the *slm1,2* mutant (data not shown) (14). Overexpression of *ROM2* or

FIGURE 4. **SLM1 is a target of calcineurin.** *A*, CNA1 and SLM1 interact in a calcineurin-sensitive manner. Cells expressing epitope-tagged CNA1 (*CNA1-HA*) (JM229), SLM1 (*SLM1-Myc*) (RL146-7d), co-expressing both tagged proteins (JM259 and JM491) or co-expressing epitope-tagged CNA1 with an epitope-tagged version of SLM1 (SLM1$^{\Delta C14}$) lacking the C-terminal 14 amino acids (*SLM1$^{\Delta C14}$-Myc*) (JM624), were grown to mid-logarithmic phase, harvested, lysed, and cell extracts were subjected to immunoprecipitation with anti-HA (*IP: CNA1*). Immunoprecipitates were probed with anti-Myc to detect coimmunoprecipitated SLM1 protein (*coIP: SLM1*). CNA1 and SLM1 interact only in a *cnb1* mutant. *B*, calcineurin dephosphorylates SLM1 *in vivo*. SLM1-TAP (RL209), SLM1-TAP *cnb1* (JM333), SLM1$^{\Delta C14}$-TAP (JM597), and SLM1$^{\Delta C14}$-TAP *cnb1* (JM712) cells were grown to mid-logarithmic phase and either mock-treated or treated with 200 mM CaCl$_2$ for 10 min. Cells were harvested and subjected to protein extraction and TAP purification, SDS-PAGE, and immunoblotting. The immunoblotting was performed with an anti-TAP (protein A) antibody to detect total SLM1-TAP (SLM1) or SLM1$^{\Delta C14}$-TAP (SLM1$^{\Delta C14}$) or with a mixture of commercial antibodies against phosphorylated serine and phosphorylated threonine to detect phospho-SLM1-TAP (*SLM1-pS/T*) or phospho-SLM1$^{\Delta C14}$-TAP (*SLM1$^{\Delta C14}$-pS/T*) (see "Experimental Procedures"). *C*, calcineurin dephosphorylates phospho-SLM1 *in vitro*. Phospho-SLM1-TAP (*SLM1-pS/T*) was purified from *cnb1* cells (JM333) and treated with recombinant calcineurin (plus calmodulin), CaCl$_2$, and EGTA as indicated and described under "Experimental Procedures." SLM1-pS/T and total SLM1-TAP (SLM1) were detected as described above.

We detected a physical interaction between SLM1 and the calcineurin catalytic subunit CNA1 but only in the absence of calcineurin activity (see above). The observation that only inactive CNA1 forms a stable complex with SLM1 suggests that calcineurin may dephosphorylate SLM1. To investigate whether calcineurin dephosphorylates SLM1, we examined the phosphorylation status of SLM1 and SLM1$^{\Delta C14}$ in wild type and *cnb1* mutant cells, treated and untreated with calcium. Affinity (TAP)-tagged SLM1 and SLM1$^{\Delta C14}$ were purified and then probed with anti-phosphoSer/Thr antibody. SLM1 was hyper-

phosphorylated in the *cnb1* mutant compared with in a wild type strain (Fig. 4*B*). SLM1$^{\Delta C14}$, consistent with its inability to interact with calcineurin, was hyperphosphorylated under all conditions examined (Fig. 4*B*). These findings suggest that calcineurin dephosphorylates SLM1 *in vivo*. Furthermore, recombinant calcineurin (plus calmodulin) dephosphorylated purified phospho-SLM1-TAP *in vitro* (Fig. 4*C*). This observation, combined with the previous observation that SLM1 physically interacts with calcineurin, suggests that calcineurin dephosphorylates SLM1 directly.

To investigate the functional consequence of SLM1 hyperphosphoryation, we examined the interaction between SLM1 and TORC2 in wild type and *cnb1* mutant cells. The TORC2-SLM interaction is weak (13, 14) and undetectable in our experimental conditions, as assayed by coimmunoprecipitation of SLM1 with AVO3 or TOR2 (Fig. 5, *A* and *B*). Inhibition of calcineurin, upon introduction of a *cnb1* mutation or treatment of cells with FK506, significantly enhanced the binding of SLM1 to both AVO3 and TOR2 (Fig. 5, *A* and *B*) (data not shown for FK506). Furthermore, the SLM1$^{\Delta C14}$ variant that was unable to bind calcineurin also exhibited enhanced binding to AVO3 and TOR2 (Fig. 5, *A* and *B*). Thus, calcineurin both dephosphorylates SLM1 and inhibits the TORC2-SLM1 interaction, suggesting that calcineurin antagonizes TORC2-SLM signaling.

To investigate further the physiological significance of SLM1 phosphorylation, we performed a more extensive phenotypic analysis of the *SLM1$^{\Delta C14}$ slm2* mutant, which grew like wild type under normal growth conditions. The *SLM1$^{\Delta C14}$ slm2* mutant was exposed to various stress conditions, including heat (37 °C), cold (15 °C), osmotic (1.8 M sorbitol or 1 M NaCl), lithium (0.3 M), calcium (0.2 M CaCl$_2$), and oxidative (5 mM H$_2$O$_2$) stress. The *SLM1$^{\Delta C14}$ slm2* was hypersensitive specifically to oxidative stress, as evidenced by a growth defect only in the presence of H$_2$O$_2$ (Fig. 5*C* and data not shown). Thus, phosphorylated SLM1 prevents the cellular response to oxidative stress, suggesting that TORC2-SLM signaling inhibits the response to this stress. In other words, calcineurin inhibits the ability of TORC2-SLM signaling to keep the response to oxidative stress at bay. A *crz1* mutation failed to confer hypersensitivity to oxidative stress, indicating that TORC2-SLM2 signaling inhibited the response to oxidative stress independently of CRZ1-dependent transcription.

DISCUSSION

We have presented evidence that TORC2-SLM signaling inhibits calcineurin, and conversely, calcineurin inhibits TORC2-SLM signaling. According to this model (Fig. 6), TORC2 phosphorylated the SLM proteins (13, 14) and thereby inhibited calcineurin and calcineurin-mediated events such as actin cytoskeleton depolarization and CRZ1-dependent transcription. Conversely, calcineurin dephosphorylates the SLMs and thereby inhibits TORC2-SLM signaling to the oxidative stress response and possibly other effectors. Thus, TORC2 and calcineurin are mutually antagonistic. The logic of this mutual antagonism may be the need to cope with the conflicting states of growth and stress. TORC2 prevents the calcineurin-activated stress response during favorable conditions, and conversely, calcineurin prevents TOR-mediated growth during
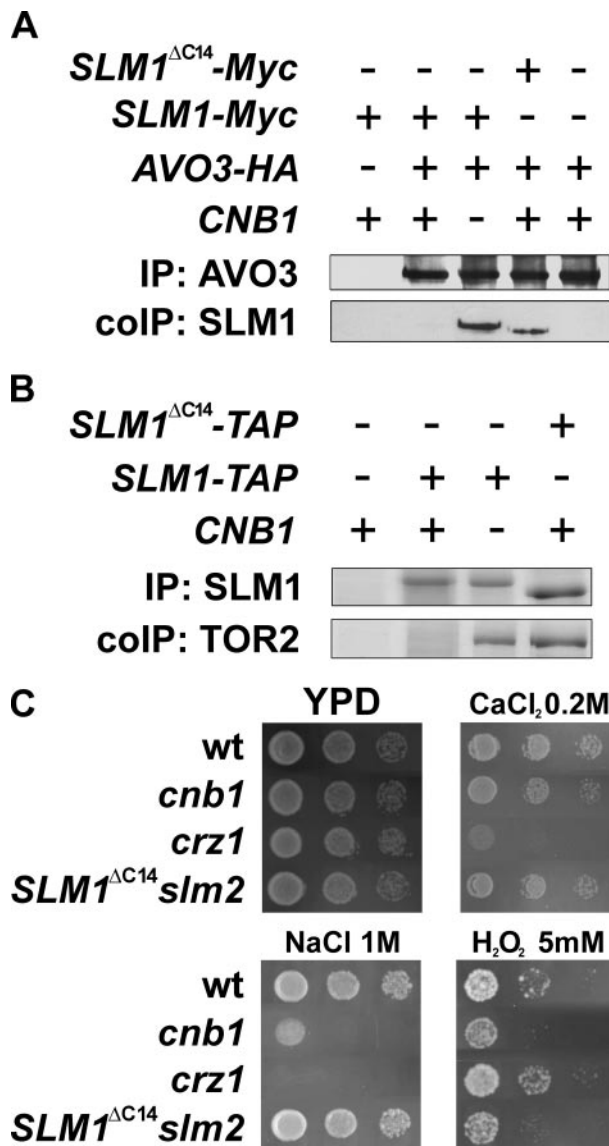
FIGURE 5. **Calcineurin inhibits the interaction between TORC2 and SLM1.** *A*, interaction of TORC2 component AVO3 with SLM1 is calcineurin-sensitive. Cells expressing epitope-tagged AVO3 (*AVO3-HA*) (RL42-1c), SLM1 (*SLM1-Myc*) (RL146-7d), both (RL164-2b and JM491), or AVO3 and an epitope-tagged version of SLM1$^{\Delta C14}$ (*SLM1$^{\Delta C14}$-Myc*) (JM626) were grown to mid-logarithmic phase, harvested, and lysed, and cell extracts were subjected to immunoprecipitation with anti-HA (*IP: AVO3*). Immunoprecipitates were probed with anti-Myc to detect coimmunoprecipitated SLM1 protein (*coIP: SLM1*). AVO3 and SLM1 interacted in a *cnb1* mutant, or when the 14 C-terminal residues of SLM1 were deleted. *B*, interaction of TOR2 with SLM1 is calcineurin-sensitive. Lysates from wild type (mock purification), SLM1-TAP (RL209), SLM1-TAP *cnb1* (JM333), and SLM1$^{\Delta C14}$-TAP (JM597) strains were subjected to TAP purification (*IP: SLM1*). Proteins were separated in a 5–20% gradient gel and stained with coomassie. TOR2 (*coIP: TOR2*) and SLM1 were identified by mass spectrometry. TOR2 and SLM1 interacted in a *cnb1* mutant, or when the C terminus of SLM1 was truncated. *C*, *SLM1$^{\Delta C14}$ slm2* is sensitive to hydrogen peroxide. The indicated strains wt (RL209), *cnb1* (JM333), *crz1* (JM717), and *SLM1$^{\Delta C14}$ slm2* (JM611) were grown to saturation in rich medium, serially diluted in water (1/10, 1/100, and 1/1000), and spotted on YPD agar or YPD agar containing the indicated compound. Growth was recorded after 48 to 72 h of incubation at 30 °C.

stress. The inhibition of calcineurin by TORC2 also allows a cell to resume growth after a stress has been overcome. Finally, another noteworthy aspect of the model (Fig. 6), which is suggested by our finding that a *cnb1* mutation suppresses the *slm1,2* actin defect, is that the SLMs mediate actin cytoskeleton
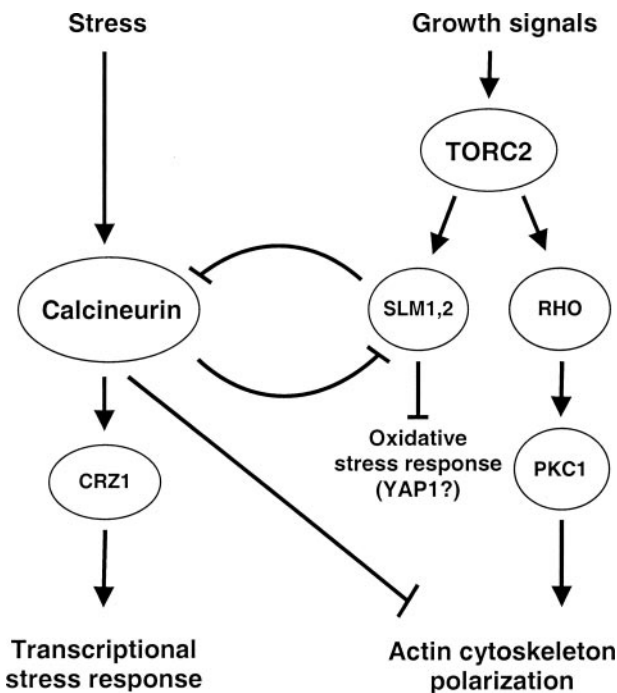

FIGURE 6. **Model for mutual antagonism TORC2 and calcineurin signaling.** Stress induces a rise in cytoplasmic calcium that activates calcineurin. Activated calcineurin dephosphorylates the SLM proteins and CRZ1. Calcineurin-mediated dephosphorylation of SLM disrupts signaling to the oxidative stress response and possibly other targets. In the absence of stress, TORC2 signals through the SLMs to control calcineurin and the oxidative stress response. SLM1,2 is required to block calcineurin signaling in normal growth conditions.

polarization via inhibition of calcineurin. The observation that the *SLM1$^{\Delta C14}$* mutation has no effect on the actin cytoskeleton (data not shown) is further evidence for this notion. Although not shown in our model, the pleckstrin homology domain-containing SLM proteins also respond to the phosphatidylinositol-4-phosphate 5-kinase MSS4 (13, 14).

Is the mutual antagonism of calcineurin and TORC2-SLM direct or indirect? The observations that calcineurin binds the SLMs, and that calcineurin dephosphorylates SLM1 *in vivo* and *in vitro* suggest that calcineurin inhibits TORC2-SLM signaling by acting on SLM directly. The mechanism of inhibition in the other direction by which TORC2-SLM inhibits calcineurin is less clear. It seems unlikely that TORC2-SLM inhibits calcineurin directly because SLM1 in the *SLM1$^{\Delta C14}$ slm2* mutant is unable to bind calcineurin, and yet this mutant grows normally and is thus still able to inhibit calcineurin. Furthermore, the observation that the *SLM1$^{\Delta C14}$ slm2* mutant responds normally to salt stress (*i.e.* calcineurin activation) suggests that SLM dephosphorylation by calcineurin is not required to activate calcineurin. How might TORC2-SLM inhibit calcineurin indirectly? We were unable to detect a change in the concentration of cytoplasmic calcium in *tor2* and *avo3* mutants, as assayed with a calcium-specific dye (Fluo-3 AM) (data not shown), suggesting that TORC2-SLM inhibits calcineurin by a mechanism other than the modulation of cytoplasmic calcium. Another possibility is that TORC2-SLM modulates the activity of the calcineurin regulator RCN1 (26). Indeed, *RCN1* transcription is up-regulated in the *tor2^{ts}* mutant at nonpermissive

temperature (Fig. 1). The mechanism by which TORC2-SLM inhibits calcineurin remains to be determined.

We present evidence that TORC2 inhibits calcineurin/CRZ1-dependent transcription and the oxidative stress response. Furthermore, TORC2 seems to control these two new readouts independently of the previously characterized RHO-PKC1-MPK1 effector pathway (Fig. 6). Although TORC1 has been known for some time to control several cellular processes via different effector pathways, TORC2 was thought to signal only to the actin cytoskeleton and only via the RHO-PKC-MPK1 pathway. TORC2, like TORC1, now appears to have multiple effectors and targets. The complexity of TORC2 signaling has been underestimated possibly because TORC2 is rapamycin-insensitive, and studies on TOR function have usually relied on rapamycin to inhibit TOR signaling. Interestingly, an important aspect of TORC1 signaling in both yeast and mammalian cells is the inhibition of type 2A and type 2A-related phosphatases (27). Our observations suggest that TORC2 also signals via inhibition of a phosphatase, in this case calcineurin.

How does TORC2-SLM signaling inhibit the oxidative stress response? Yokoyama *et al.* (28) have suggested that YAP1, a transcription factor mediating the oxidative stress response, is controlled by calcineurin. Thus, an appealing model is that TORC2-SLM signaling inhibits the oxidative stress response by inhibiting YAP1. In the absence of stress, SLM is phosphorylated and bound to TORC2 and could thereby serve as an adaptor presenting YAP1 to TORC2 for phosphorylation and inhibition. Alternatively, as YAP1 is regulated at the level of nuclear localization, phosphorylated SLM could simply bind and sequester YAP1. In response to stress, calcineurin dephosphorylates SLM and possibly YAP1, leading to activation of YAP1. Interestingly, at least three CRZ1-independent YAP1 target genes (*CTT1*, *ARG4*, and *LAP4*) are up-regulated in the *tor2^{ts}* mutant at nonpermissive temperature (www.ncbi.nlm.nih.gov/geo/; accession number GSE1814). It is also interesting to note that TOR controls nuclear localization of several stress-related transcription factors, including GLN3, GAT1, MSN2/4, RTG1, RTG3, and as shown here, CRZ1 (15, 29, 30).

Does mTOR inhibit calcineurin in mammalian cells? mTOR promotes skeletal myotube hypertrophy in response to insulin-like growth factor-1, and this effect is enhanced by the calcineurin inhibitor cyclosporin A (31). Furthermore, mTORC2 mediates actin polymerization in mammalian cells (32, 33), and calcineurin induces F-actin destabilization in dendritic spines (34). Thus, mTORC2 may inhibit calcineurin also in mammalian cells. mTORC2 signaling, which like TORC2 signaling in yeast is rapamycin-insensitive, probably has a broader role in the control of cell growth than commonly appreciated.

REFERENCES

1. Loewith, R., Jacinto, E., Wullschleger, S., Lorberg, A., Crespo, J. L., Bonenfant, D., Oppliger, W., Jenoe, P., and Hall, M. N. (2002) *Mol. Cell* **10,** 457–468
2. Wedaman, K. P., Reinke, A., Anderson, S., Yates, J., 3rd, McCaffery, J. M., and Powers, T. (2003) *Mol. Biol. Cell* **14,** 1204–1220
3. Wullschleger, S., Loewith, R., and Hall, M. N. (2006) *Cell* **124,** 471–484
4. Schmidt, A., Bickle, M., Beck, T., and Hall, M. N. (1997) *Cell* **88,** 531–542
5. Helliwell, S. B., Schmidt, A., Ohya, Y., and Hall, M. N. (1998) *Curr. Biol.* **8,** 1211–1214
6. Cyert, M. S. (2001) *Annu. Rev. Genet.* **35,** 647–672
7. Stathopoulos, A. M., and Cyert, M. S. (1997) *Genes Dev.* **11,** 3432–3444
8. Matheos, D. P., Kingsbury, T. J., Ahsan, U. S., and Cunningham, K. W. (1997) *Genes Dev.* **11,** 3445–3458
9. Mendizabal, I., Rios, G., Mulet, J. M., Serrano, R., and de Larrinoa, I. F. (1998) *FEBS Lett.* **425,** 323–328
10. Mizunuma, M., Hirata, D., Miyahara, K., Tsuchiya, E., and Miyakawa, T. (1998) *Nature* **392,** 303–306
11. Shitamukai, A., Hirata, D., Sonobe, S., and Miyakawa, T. (2004) *J. Biol. Chem.* **279,** 3651–3661
12. Uetz, P., Giot, L., Cagney, G., Mansfield, T. A., Judson, R. S., Knight, J. R., Lockshon, D., Narayan, V., Srinivasan, M., Pochart, P., Qureshi-Emili, A., Li, Y., Godwin, B., Conover, D., Kalbfleisch, T., Vijayadamodar, G., Yang, M., Johnston, M., Fields, S., and Rothberg, J. M. (2000) *Nature* **403,** 623–627
13. Audhya, A., Loewith, R., Parsons, A. B., Gao, L., Tabuchi, M., Zhou, H., Boone, C., Hall, M. N., and Emr, S. D. (2004) *EMBO J.* **23,** 3747–3757
14. Fadri, M., Daquinag, A., Wang, S., Xue, T., and Kunz, J. (2005) *Mol. Biol. Cell* **16,** 1883–1900
15. Beck, T., and Hall, M. N. (1999) *Nature* **402,** 689–692
16. Sherman, F. (1991) *Methods Enzymol.* **194,** 3–21
17. Wullschleger, S., Loewith, R., Oppliger, W., and Hall, M. N. (2005) *J. Biol. Chem.* **280,** 30697–30704
18. Longtine, M. S., McKenzie, A., 3rd, Demarini, D. J., Shah, N. G., Wach, A., Brachat, A., Philippsen, P., and Pringle, J. R. (1998) *Yeast* **14,** 953–961
19. Helliwell, S. B., Howald, I., Barbet, N., and Hall, M. N. (1998) *Genetics* **148,** 99–112
20. Martin, D. E., Demougin, P., Hall, M. N., and Bellis, M. (2004) *BMC Bioinformatics* **5,** 148
21. Schmitt, M. E., Brown, T. A., and Trumpower, B. L. (1990) *Nucleic Acids Res.* **18,** 3091–3092
22. Heath, V. L., Shaw, S. L., Roy, S., and Cyert, M. S. (2004) *Eukaryot. Cell* **3,** 695–704
23. Schmelzle, T., Beck, T., Martin, D. E., and Hall, M. N. (2004) *Mol. Cell. Biol.* **24,** 338–351
24. Yoshimoto, H., Saltsman, K., Gasch, A. P., Li, H. X., Ogawa, N., Botstein, D., Brown, P. O., and Cyert, M. S. (2002) *J. Biol. Chem.* **277,** 31079–31088
25. Stathopoulos-Gerontides, A., Guo, J. J., and Cyert, M. S. (1999) *Genes Dev.* **13,** 798–803
26. Kingsbury, T. J., and Cunningham, K. W. (2000) *Genes Dev.* **14,** 1595–1604
27. Jacinto, E., and Hall, M. N. (2003) *Nat. Rev. Mol. Cell Biol.* **4,** 117–126
28. Yokoyama, H., Mizunuma, M., Okamoto, M., Yamamoto, J., Hirata, D., and Miyakawa, T. (2006) *EMBO Rep.* **7,** 519–524
29. Komeili, A., Wedaman, K. P., O'Shea, E. K., and Powers, T. (2000) *J. Cell Biol.* **151,** 863–878
30. Crespo, J. L., Powers, T., Fowler, B., and Hall, M. N. (2002) *Proc. Natl. Acad. Sci. U. S. A.* **99,** 6784–6789
31. Rommel, C., Bodine, S. C., Clarke, B. A., Rossman, R., Nunez, L., Stitt, T. N., Yancopoulos, G. D., and Glass, D. J. (2001) *Nat. Cell Biol.* **3,** 1009–1013
32. Jacinto, E., Loewith, R., Schmidt, A., Lin, S., Ruegg, M. A., Hall, A., and Hall, M. N. (2004) *Nat. Cell Biol.* **6,** 1122–1128
33. Sarbassov, D. D., Ali, S. M., Kim, D. H., Guertin, D. A., Latek, R. R., Erdjument-Bromage, H., Tempst, P., and Sabatini, D. M. (2004) *Curr. Biol.* **14,** 1296–1302
34. Halpain, S., Hipolito, A., and Saffer, L. (1998) *J. Neurosci.* **18,** 9835–9844

Mutual Antagonism of Target of Rapamycin and Calcineurin Signaling

Jose M. Mulet, Dietmar E. Martin, Robbie Loewith and Michael N. Hall

Access the most updated version of this article at doi: 10.1074/jbc.M604244200

Alerts:

- When this article is cited
- When a correction for this article is posted

Click here to choose from all of JBC's e-mail alerts

This article cites 34 references, 16 of which can be accessed free at
http://www.jbc.org/content/281/44/33000.full.html#ref-list-1